Check for updates

Thermodynamic evaluations of the acceptorless dehydrogenation and hydrogenation of pre-aromatic and aromatic N-heterocycles in acetonitrile

Bao-Chen Qian,[a] Xiao Wang,[a] Qi Wang,[a] Xiao-Qing Zhu[*b] and Guang-Bin Shen [ID] [*a]

N-heterocycles are important chemical hydrogen-storage materials, and the acceptorless dehydrogenation and hydrogenation of N-heterocycles as organic hydrogen carriers have been widely studied, with the main focus on the catalyst synthesis and design, investigation of the redox mechanisms, and extension of substrate scope. In this work, the Gibbs free energies of the dehydrogenation of pre-aromatic N-heterocycles ($\mathbf{YH_2}$) and the hydrogenation of aromatic N-heterocycles ($\mathbf{Y}$), *i.e.*, $\Delta G_{H_2R}(\mathbf{YH_2})$ and $\Delta G_{H_2A}(\mathbf{Y})$, were derived by constructing thermodynamic cycles using Hess' law. The thermodynamic abilities for the acceptorless dehydrogenation and hydrogenation of 78 pre-aromatic N-heterocycles ($\mathbf{YH_2}$) and related 78 aromatic N-heterocycles ($\mathbf{Y}$) were well evaluated and discussed in acetonitrile. Moreover, the applications of the two thermodynamic parameters in identifying pre-aromatic N-heterocycles possessing reversible dehydrogenation and hydrogenation properties and the selection of the pre-aromatic N-heterocyclic hydrogen reductants in catalytic hydrogenation were considered and are discussed in detail. Undoubtedly, this work focuses on two new thermodynamic parameters of pre-aromatic and aromatic N-heterocycles, namely $\Delta G_{H_2R}(\mathbf{YH_2})$ and $\Delta G_{H_2A}(\mathbf{Y})$, which are important supplements to our previous work to offer precise insights into the chemical hydrogen storage and hydrogenation reactions of pre-aromatic and aromatic N-heterocycles.

1 Introduction

The acceptorless dehydrogenation and hydrogenation of N-heterocycles are key atom-economical and fundamental methods to afford various imine and amine derivatives with potential bioactivities.[1–11] Additionally, the two kinds of redox reactions, especially the reversible acceptorless dehydrogenation and hydrogenation of N-heterocycles, involve the release and acceptance of H_2, which indicate that N-heterocycles are significant chemical hydrogen-storage materials. In fact, N-heterocycles have already been verified as an important type of chemical hydrogen-storage materials.[12–19] The acceptorless dehydrogenation and hydrogenation of N-heterocycles as organic hydrogen carriers have been broadly studied, mainly focusing on the catalyst synthesis and design, investigation of the redox mechanisms, and extension of substrate scope.[3–19]

Since the chemical processes for the acceptorless dehydrogenation and hydrogenation of N-heterocycles involve H_2 release and acceptance, therefore, the thermodynamics of the dehydrogenation and hydrogenation of N-heterocycles are important thermodynamic parameters to evaluate the hydrogen-storage abilities and hydrogenation abilities of N-heterocycles, especially for pre-aromatic N-heterocycles possessing reversible dehydrogenation and hydrogenation abilities.[3–8] This work follows on from our previous study into the thermodynamics of hydrogen transfer for amines.[20] This present work focuses on thermodynamic evaluations of the acceptorless dehydrogenation and hydrogenation of a special category of N-heterocycles, namely, pre-aromatic and aromatic N-heterocycles, in acetonitrile.

In our previous research work, we computed the Gibbs free energies of 84 amines ($\mathbf{YH_2}$), including 78 pre-aromatic N-heterocycles and 6 general amines, releasing hydrides and their activation free energies for hydride self-exchange reactions, *i.e.*, $\Delta G_{H-R}(\mathbf{YH_2})$ and $\Delta G^{\ddagger}(\mathbf{YH_2}/\mathbf{YH^+})$, using density functional theory (DFT) calculations in acetonitrile.[20a] Earlier in 2023, thermodynamic evaluations were conducted of 84 amines releasing two hydrogen ions ($H^- + H^+$) and the corresponding 84 imines accepting two hydrogen ions ($H^- + H^+$), including $\Delta G_{H-PR}(\mathbf{YH_2})$ and $\Delta G_{H-PA}(\mathbf{Y})$.[20b] Combined with the above thermodynamic data, in this work, the thermodynamic values upon H_2 release and acceptance for the dehydrogenation and hydrogenation of pre-aromatic and aromatic N-heterocycles

[a]*College of Medical Engineering, Jining Medical University, Jining, Shandong, 272000, P. R. China. E-mail: gbshen@mail.jnmc.edu.cn*

[b]*The State Key Laboratory of Elemento-Organic Chemistry, Department of Chemistry, Nankai University, Tianjin 300071, China. E-mail: xqzhu@nankai.edu.cn*

(Scheme 1) were naturally derived *via* constructing thermodynamic cycles using Hess' law,[21] and the thermodynamic abilities of the pre-aromatic N-heterocycles as chemical hydrogen-storage materials were well evaluated and compared. Moreover, application of the thermodynamic data for identifying pre-aromatic N-heterocycles possessing reversible dehydrogenation and hydrogenation abilities[3–8] were investigated and discussed in detail. Undoubtedly, this work focuses on new thermodynamic parameters, which is an important supplement to our previous work to offer precise insights into the chemical hydrogen storage and hydrogenation reactions of pre-aromatic N-heterocycles.[1–19]

2   Results and discussion

In this work, 78 various pre-aromatic N-heterocycles ($1H_2$–$78H_2$) were designed to expand the scope of the investigated N-heterocyclic substrates, and 6 general amines ($79H_2$–$84H_2$) were designed for comparison with pre-aromatic N-heterocycles. The chemical structures of 84 amines (YH_2), including the 78 pre-aromatic N-heterocycles ($1H_2$–$78H_2$) and 6 general amines ($79H_2$–$84H_2$), are shown in Scheme 2.

To obtain the Gibbs free energy of YH_2 releasing H_2, the constructed thermodynamic cycle based on the processes of YH_2 releasing two hydrogen ions or H_2 in acetonitrile is shown in Scheme 3. As can be seen from Scheme 3, Step 1 is the chemical process of YH_2 releasing H_2, $YH_2 \rightarrow Y + H_2$, and the thermodynamic driving force of YH_2 dehydrogenation could be described by the Gibbs free energy of YH_2 releasing H_2, $\Delta G_{H_2R}(YH_2)$. Step 2 is the chemical process of YH_2 releasing two hydrogen ions, $YH_2 \rightarrow Y + H^- + H^+$, and the corresponding thermodynamic driving force was defined as the Gibbs free energy of YH_2 releasing two hydrogen ions, $\Delta G_{H^-PR}(YH_2)$.[20] Step 3 is the chemical process of H^- reacting with H^+ to form H_2, $H^- + H^+ \rightarrow H_2$, and the related thermodynamic driving force was defined as the Gibbs free energy of one molar H^- reacting with one molar H^+ to generate one molar H_2, $\Delta G_{PA}(H^-)$. The $\Delta G_{PA}(H^-)$ value was reported as −76.0 kcal mol^{-1} in acetonitrile.[22–24] Therefore, the value of $\Delta G_{H_2R}(YH_2)$ could be calculated using eqn (1) in Table 1 by establishing a thermodynamic cycle according to Hess' law (Scheme 3),[21] where $\Delta G_{H_2R}(YH_2) = \Delta G_{H^-PR}(YH_2) + \Delta G_{PA}(H^-)$ (eqn (1)). For eqn (1), $\Delta G_{H^-PR}(YH_2)$ values are available from our previous work and are displayed in the fourth column of Table 2. Since the $\Delta G_{H^-R}(YH_2)$ values were computed using the DFT method with

a precision of 1.1 kcal mol^{-1} in our previous work,[20a] and the pK_a values of YH$^+$ were predicted using XGBoost with a 0.87 pK_a error,[20a] the $\Delta G_{H_2R}(YH_2)$ values were derived from $\Delta G_{H^-R}(YH_2)$ and pK_a(YH$^+$), whereby $\Delta G_{H_2R}(YH_2) = \Delta G_{H^-R}(YH_2) + 1.37pK_a$(YH$^+$), and therefore, the precision of the $\Delta G_{H_2R}(YH_2)$ values could be estimated within 2.3 kcal mol^{-1}, which was a suitable precision to give practical guidance on the chemical hydrogen storage and hydrogenation reactions, *etc.*

Step 4 in Scheme 2 is the chemical process of Y accepting H_2 to offer YH_2, $Y + H_2 \rightarrow YH_2$, and the corresponding thermodynamic driving force could be described as the Gibbs free energy of Y accepting H_2 to generate YH_2, $\Delta G_{H_2A}(Y)$. Since the Y hydrogenation and YH_2 dehydrogenation are reverse chemical reactions, the $\Delta G_{H_2A}(Y)$ value was the opposite of the $\Delta G_{H_2R}(YH_2)$ value,[21] *i.e.*, $\Delta G_{H_2A}(Y) = -\Delta G_{H_2R}(YH_2)$ (eqn (2) in Table 1). Herein, the chemical processes, thermodynamic parameters, and data sources or computed equations of step 1–step 4 for YH_2 dehydrogenation and Y hydrogenation in acetonitrile are presented in Table 1, meanwhile, the $\Delta G_{H^-PR}(YH_2)$, $\Delta G_{H^-PA}(Y)$, $\Delta G_{H_2R}(YH_2)$, and $\Delta G_{H_2A}(Y)$ values of the 84 amines (YH_2) dehydrogenation and their relevant imines (Y) hydrogenation in acetonitrile are listed in Table 2.

2.1.   Thermodynamic abilities of YH_2 dehydrogenation as organic hydrogen-storage materials

For better comparing the relationship between the thermodynamic abilities and chemical structures, all 84 amines (YH_2) were divided into 4 groups,[20] comprising 1,4-dihydropyridine compounds (Y_IH_2, $1H_2$–$62H_2$), 1,2-dihydropyridines ($Y_{II}H_2$, $63H_2$–$73H_2$), 1,2-dihydro-3-substituted-indoline analogs ($Y_{III}H$, $74H_2$–$78H_2$), and general amines ($Y_{IV}H_2$, $79H_2$–$84H_2$) (Scheme 4). Among the 4 groups, Y_IH_2, $Y_{II}H_2$, and $Y_{III}H_2$ were 1,4-dihydro nitric six-member heterocycles, 1,2-dihydro nitric six-member heterocycles, and 1,2-dihydro nitric five-member heterocycles, respectively, which all belong to pre-aromatic N-heterocycles. As pre-aromatic N-heterocycles, the resulting dehydrogenation products Y (Y_I, Y_{II}, and Y_{III}) are aromatic N-heterocycles (Scheme 4) after YH_2 releases H_2, $YH_2 \rightarrow Y + H_2$.

According to the definition of $\Delta G_{H_2R}(YH_2)$, if the $\Delta G_{H_2R}(YH_2)$ value is more negative than 0, $\Delta G_{H_2R}(YH_2) < 0$, the chemical process of YH_2 releasing H_2 is thermodynamically favorable, and YH_2 is recognized as a thermodynamically excellent H_2 donor.[21] In contrast, if the $\Delta G_{H_2R}(YH_2)$ value is greater than 0, $\Delta G_{H_2R}(YH_2) > 0$, the chemical process of YH_2 releasing H_2 is thermodynamically unfavorable, and YH_2 is not a thermodynamically feasible H_2 donor.

As can be seen from Table 2, the $\Delta G_{H_2R}(YH_2)$ scale of the 78 pre-aromatic N-heterocycles ($1H_2$–$78H_2$) investigated in this work ranged from −15.8 kcal mol^{-1} to 22.0 kcal mol^{-1}, which spanned a very wide thermodynamic range of 37.8 kcal mol^{-1}. Moreover, among the 78 pre-aromatic N-heterocycles ($1H_2$–$78H_2$), $21H_2$ from Y_IH_2 was thermodynamically the best hydrogen donor or carrier (−15.8 kcal mol^{-1}), even better than HCO$_2$H (−5.9 kcal mol^{-1}),[25] while $44H_2$ from Y_IH_2 was thermodynamically the worst hydrogen donor or carrier (22.0 kcal mol^{-1}). For more refined thermodynamic analysis,
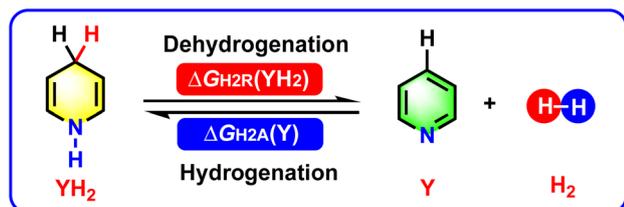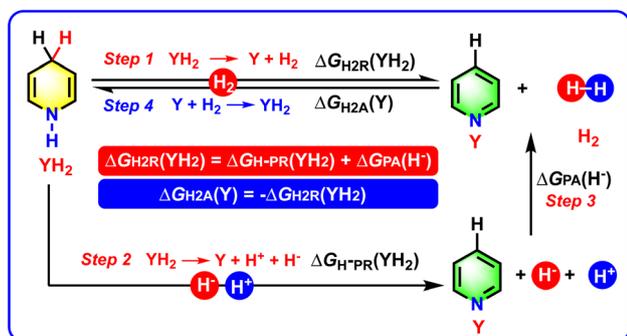

Scheme 1 Chemical equations for the acceptorless dehydrogenation and hydrogenation of pre-aromatic and aromatic N-heterocycles.
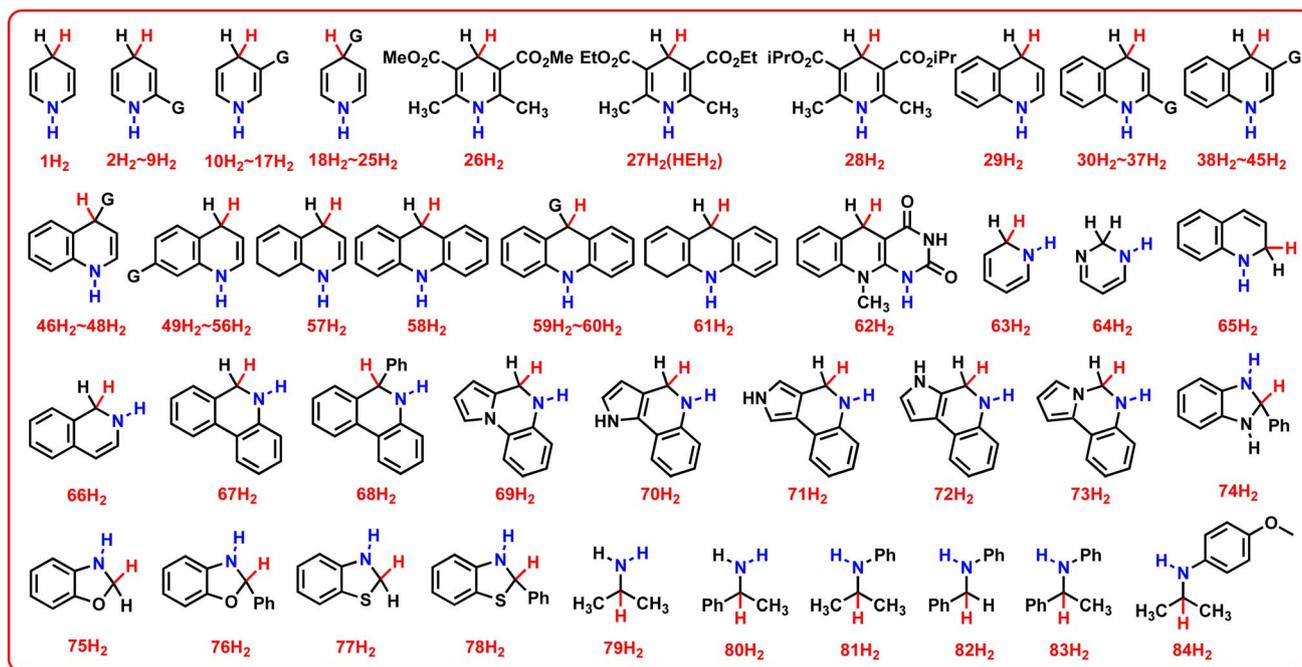
Scheme 2 Chemical structures of 84 amines (YH$_2$), including the 78 pre-aromatic N-heterocycles (1H$_2$–78H$_2$) and 6 general amines (79H$_2$–84H$_2$) investigated in this work.

Scheme 3 Constructed thermodynamic cycle based on the processes of YH$_2$ releasing two hydrogen ions or H$_2$ in acetonitrile.

the distribution of $\Delta G_{H_2R}(YH_2)$ values for the 78 pre-aromatic N-heterocycles (1H$_2$–78H$_2$) in every 5 kcal mol^{-1} is clearly shown in Fig. 1 with YH$_2$ amounts as the ordinate and $\Delta G_{H_2R}(YH_2)$ ranges as the abscissa.

From Fig. 1, several interesting conclusions could be drawn as follows. (1) The distribution of YH$_2$ amounts exhibited an excellent normal distribution, and $\Delta G_{H_2R}(YH_2)$ values of pre-aromatic N-heterocycles ranging from 0 to 5 kcal mol^{-1} were the most common (29.5%). (2) It was found that the $\Delta G_{H_2R}(YH_2)$ values of 30 YH$_2$ were more negative than 0, meaning that 30 YH$_2$ were thermodynamically feasible H$_2$ donors, and belonged to potential chemical hydrogen-storage materials. While the $\Delta G_{H_2R}(YH_2)$ values of 48 YH$_2$ were greater than 0, indicating that the 48 YH$_2$ were thermodynamically unfeasible H$_2$ donors. (3) It was also discovered that 75 $\Delta G_{H_2R}(YH_2)$ values ranged from −15 kcal mol^{-1} to 15 kcal mol^{-1}, indicating that ∼96% of the thermodynamic driving forces for the pre-aromatic N-heterocycles dehydrogenations were between −15 kcal mol^{-1} to 15 kcal mol^{-1}, while less than 4% of the thermodynamic driving forces for the pre-aromatic N-heterocycles dehydrogenation were more negative than −15 kcal mol^{-1} or greater than 15 kcal mol^{-1}. Accordingly, for an unknown pre-aromatic N-heterocycle, the thermodynamic driving force for YH$_2$ dehydrogenation is generally between −15 kcal mol^{-1} to 15 kcal mol^{-1} (∼96% possibilities).

Table 1 Chemical processes, thermodynamic parameters, and data sources or computed equations of step 1–step 4 for YH$_2$ dehydrogenation and Y hydrogenation in acetonitrile

Chemical processes		Thermodynamic parameters	Sources or computed equations	Equation X
Step 1	YH$_2$ → Y + H$_2$	$\Delta G_{H_2R}(YH_2)$	$\Delta G_{H_2R}(YH_2) = \Delta G_{H^-PR}(YH_2) + \Delta G_{PA}(H^-)$	1
Step 2	YH$_2$ → Y + H$^-$ + H$^+$	$\Delta G_{H^-PR}(YH_2)$	Ref. 20	—
Step 3	H$^-$ + H$^+$ → H$_2$	$\Delta G_{PA}(H^-)$	−76.0 kcal mol^{-1} (ref. 22–24)	—
Step 4	Y + H$_2$ → YH$_2$	$\Delta G_{H_2A}(Y)$	$\Delta G_{H_2A}(Y) = -\Delta G_{H_2R}(YH_2)$	2

Table 2 $\Delta G_{H-PR}(YH_2)$, $\Delta G_{H-PA}(Y)$, $\Delta G_{H_2R}(YH_2)$, and $\Delta G_{H_2A}(Y)$ values of the 84 considered amines (YH$_2$) and their corresponding imines (Y) in acetonitrile (unit: kcal mol^{-1})

Compounds	Structures	G	$\Delta G_{H-PR}(YH_2)^a$ / $-\Delta G_{H-PA}(Y)^a$	$\Delta G_{H_2R}(YH_2)^b$ / $-\Delta G_{H_2A}(Y)^c$
1H$_2$		—	68.0	−8.0
2H$_2$		CH$_3$	68.8	−7.2
3H$_2$		^{t}Bu	70.6	−5.4
4H$_2$		Ph	66.5	−9.5
5H$_2$		NH$_2$	63.5	−12.5
6H$_2$		CHO	75.6	−0.4
7H$_2$		CN	75.2	−0.8
8H$_2$		NO	78.9	2.9
9H$_2$		NO$_2$	71.7	−4.3
10H$_2$		CH$_3$	69.7	−6.3
11H$_2$		^{t}Bu	71.8	−4.2
12H$_2$		Ph	70.2	−5.8
13H$_2$		NH$_2$	67.8	−8.2
14H$_2$		CHO	80.6	4.6
15H$_2$		CN	78.7	2.7
16H$_2$		NO	87.3	11.3
17H$_2$		NO$_2$	85.7	9.7
18H$_2$		CH$_3$	67.4	−8.6
19H$_2$		^{t}Bu	72.0	−4.0
20H$_2$		Ph	64.8	−11.2
21H$_2$		NH$_2$	60.2	−15.8
22H$_2$		CHO	72.3	−3.7
23H$_2$		CN	74.1	−1.9
24H$_2$		NO	76.6	0.6
25H$_2$		NO$_2$	84.6	8.6
26H$_2$		—	83.1	7.1
27H$_2$		—	83.3	7.3
28H$_2$		—	83.4	7.4
29H$_2$		—	77.9	1.9
30H$_2$		CH$_3$	75.8	−0.2
31H$_2$		^{t}Bu	79.5	3.5
32H$_2$		Ph	75.9	−0.1
33H$_2$		NH$_2$	69.6	−6.4
34H$_2$		CHO	86.0	10.0
35H$_2$		CN	86.4	10.4
36H$_2$		NO	91.0	15.0
37H$_2$		NO$_2$	81.8	5.8
38H$_2$		CH$_3$	76.7	0.7
39H$_2$		^{t}Bu	81.1	5.1
40H$_2$		Ph	78.8	2.8
41H$_2$		NH$_2$	76.8	0.8
42H$_2$		CHO	89.4	13.4
43H$_2$		CN	87.3	11.3

Table 2 (*Contd.*)

Compounds	Structures	G	$\Delta G_{H-PR}(YH_2)^a$ / $-\Delta G_{H-PA}(Y)^a$	$\Delta G_{H_2R}(YH_2)^b$ / $-\Delta G_{H_2A}(Y)^c$
44H$_2$		NO	98.0	22.0
45H$_2$		NO$_2$	93.2	17.2
46H$_2$		CH$_3$	73.5	−2.5
47H$_2$		^{t}Bu	84.9	8.9
48H$_2$		Ph	74.9	−1.1
49H$_2$		CH$_3$	76.2	0.2
50H$_2$		^{t}Bu	80.1	4.1
51H$_2$		Ph	75.9	−0.1
52H$_2$		NH$_2$	74.7	−1.3
53H$_2$		CHO	79.0	3.0
54H$_2$		CN	80.6	4.6
55H$_2$		NO	80.4	4.4
56H$_2$		NO$_2$	81.2	5.2
57H$_2$		—	67.6	−8.4
58H$_2$		H	87.5	11.5
59H$_2$		CH$_3$	87.5	11.5
60H$_2$		Ph	87.3	11.3
61H$_2$		—	76.3	0.3
62H$_2$		—	87.6	11.6
63H$_2$		—	64.5	−11.5
64H$_2$		—	73.7	−2.3
65H$_2$		—	74.6	−1.4
66H$_2$		—	77.6	1.6
67H$_2$		—	79.6	3.6
68H$_2$		—	78.4	2.4

Table 2 (Contd.)

Compounds	Structures	G	$\Delta G_{H^-PR}(YH_2)^a$ $-\Delta G_{H^-PA}(Y)^a$	$\Delta G_{H_2R}(YH_2)^b$ $-\Delta G_{H_2A}(Y)^c$
69H$_2$		—	84.1	8.1
70H$_2$		—	76.6	0.6
71H$_2$		—	80.8	4.8
72H$_2$		—	77.0	1.0
73H$_2$		—	84.5	8.5
74H$_2$		—	68.6	−7.4
75H$_2$		—	85.5	9.5
76H$_2$		—	78.2	2.2
77H$_2$		—	82.7	6.7
78H$_2$		—	76.9	0.9
79H$_2$		—	86.3	10.3
80H$_2$		—	87.6	11.6
81H$_2$		—	91.2	15.2
82H$_2$		—	93.8	17.8
83H$_2$		—	93.7	17.7

Table 2 (Contd.)

Compounds	Structures	G	$\Delta G_{H^-PR}(YH_2)^a$ $-\Delta G_{H^-PA}(Y)^a$	$\Delta G_{H_2R}(YH_2)^b$ $-\Delta G_{H_2A}(Y)^c$
84H$_2$		—	94.3	18.3

[a] $\Delta G_{H^-PR}(YH_2)$ and $\Delta G_{H^-PA}(Y)$ values are from ref. 20. [b] $\Delta G_{H_2R}(YH_2) = \Delta G_{H^-PR}(YH_2) + \Delta G_{PA}(H^-)$. [c] $\Delta G_{H_2A}(Y) = -\Delta G_{H_2R}(YH_2)$.

To clearly reveal the relationship between the structural features and thermodynamic abilities, the $\Delta G_{H_2R}(YH_2)$ scales of 4 groups of YH_2, along with the $\Delta G_{H_2R}(XH_2)$ values of HCO$_2$H, H$_2$, 67H$_2$, 78H$_2$, and HEH$_2$ (Hantzsch ester, 27H$_2$) releasing H$_2$ in acetonitrile are shown in Scheme 5,[25–27] because HCO$_2$H,[28] H$_2$,[29–33] 67H$_2$,[34,35] 78H$_2$,[36,37] and HEH$_2$ (27H$_2$)[38–40] are the most frequently-used hydrogen reductants (denoted as XH$_2$) used in the hydrogenation reactions.

From Scheme 5, the following valuable conclusions could be made: (1) the $\Delta G_{H_2R}(Y_IH_2)$ scale covered from −15.8 kcal mol^{-1} to 22.0 kcal mol^{-1}, which spanned the widest thermodynamic range by 37.8 kcal mol^{-1} among the 4 groups of amines Y_IH_2–$Y_{IV}H_2$; (2) according to the $\Delta G_{H_2R}(YH_2)$ scales of $Y_{II}H_2$ (−11.5 to 8.5 kcal mol^{-1}), $Y_{III}H_2$ (−7.4 to 9.5 kcal mol^{-1}), and $Y_{IV}H_2$ (10.3– 18.3 kcal mol^{-1}), the dehydrogenation abilities decreased in the order of $Y_{II}H_2 \approx Y_{III}H_2 > Y_{IV}H_2$; (3) in view of the relations between sets, it was found that the $\Delta G_{H_2R}(YH_2)$ values displayed the following regular pattern of $\{\Delta G_{H_2R}(Y_{II}H_2) \cup \Delta G_{H_2R}(Y_{III}H_2) \cup \Delta G_{H_2R}(Y_{IV}H_2)\} \subseteq \Delta G_{H_2R}(Y_IH_2)$; (4) for the pre-aromatic N-heterocycles, the $\Delta G_{H_2R}(YH_2)$ scales ranged from −15.8 to 22.0 kcal mol^{-1} for Y_IH_2, from −11.5 to 8.5 kcal mol^{-1} for $Y_{II}H_2$, and from −7.4 to 9.5 kcal mol^{-1} for $Y_{III}H_2$, respectively. Since the $\Delta G_{H_2R}(YH_2)$ scales of Y_IH_2, $Y_{II}H_2$, and $Y_{III}H_2$ crossed negative and positive values (−15.8 to 22.0 kcal mol^{-1}), it was indicated that not all the acceptorless dehydrogenation of pre-aromatic N-heterocycles is a thermodynamically uphill or downhill process under ambient conditions,[3–19] and not all pre-aromatic N-heterocycles are thermodynamically feasible to serve as chemical hydrogen-storage materials. $\Delta G_{H_2R}(YH_2)$ is absolutely an important thermodynamic parameter to guide chemists to discover more potentially excellent chemical hydrogen-storage materials.

Initially, we tried to explain the effects of substituents on $\Delta G_{H_2R}(YH_2)$, but we failed to draw a meaningful conclusion. For example, an electron-withdrawing group could decrease the hydride-donating ability of YH_2, $\Delta G_{H^-R}(YH_2)$, while it increased the proton-donating ability of YH$^+$, $\Delta G_{PR}(YH^+)$. Since $\Delta G_{H_2R}(YH_2)$ is derived from $\Delta G_{H^-R}(YH_2)$ and $\Delta G_{PR}(YH^+)$ essentially, i.e., $\Delta G_{H_2R}(YH_2) = \Delta G_{H^-R}(YH_2) + \Delta G_{PR}(YH^+) + \Delta G_{PA}(H^-)$, for YH_2 possessing an electron-withdrawing group, whether the $\Delta G_{H_2R}(YH_2)$ value increases or decreases depends on the D-values of $\Delta G_{H^-R}(YH_2)$ decreasing and $\Delta G_{PR}(YH^+)$ increasing, i.e.,
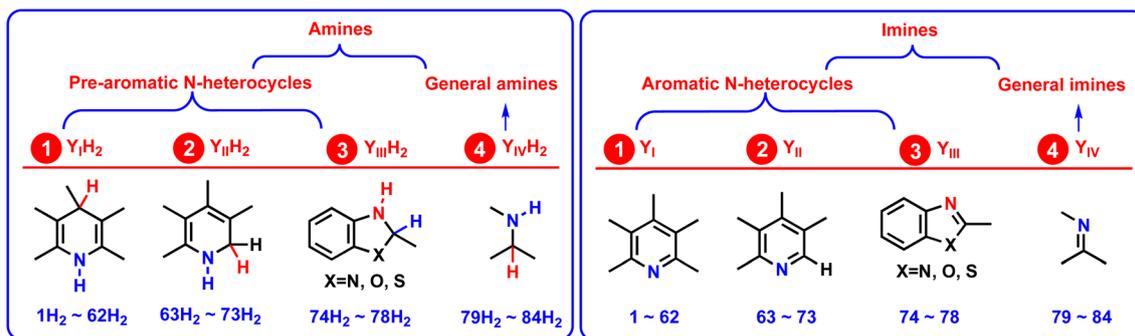
Scheme 4 Classifications of the 84 amines (YH$_2$) and imines (Y) and the corresponding 4 groups of YH$_2$ and Y, respectively, considered in this work.
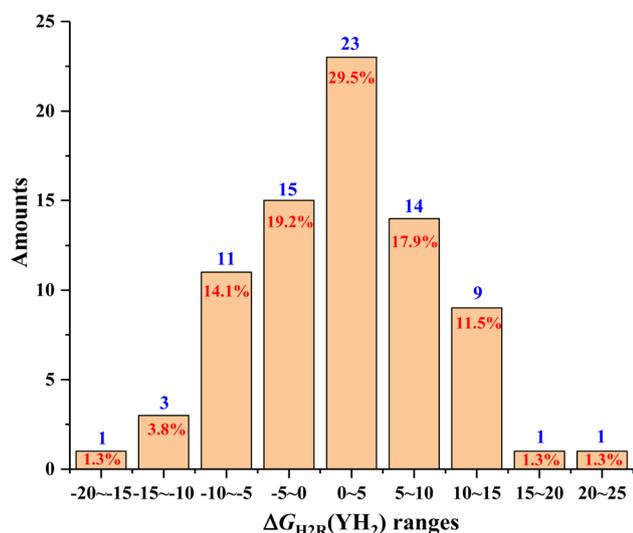

Fig. 1 Distributions of $\Delta G_{H_2R}(YH_2)$ ranges for the 78 pre-aromatic N-heterocycles in every 5 kcal mol^{-1} from -20 kcal mol^{-1} to 25 kcal mol^{-1}.

$\Delta\Delta G_{H^-R}(YH_2)$ and $\Delta\Delta G_{PR}(YH^+)$. In addition, the steric factors from the substituents will have a significant effect on reaction kinetics, and a slight effect on the reaction thermodynamics.

2.2. Thermodynamic abilities of Y hydrogenation to generate YH$_2$

According to the physical meaning of $\Delta G_{H_2A}(Y)$, if the $\Delta G_{H_2A}(Y)$ value is more negative than 0, $\Delta G_{H_2A}(Y) < 0$, the **Y** hydrogenation

by H$_2$ is thermodynamically favorable. The more negative the $\Delta G_{H_2A}(Y)$ value, the larger the thermodynamic driving force of **Y** hydrogenation by H$_2$. While if the $\Delta G_{H_2A}(Y)$ value is greater than 0, $\Delta G_{H_2A}(Y) > 0$, the **Y** hydrogenation by H$_2$ is thermodynamically unfavorable, and the larger the $\Delta G_{H_2A}(Y)$ value, the smaller the thermodynamic driving force of **Y** hydrogenation by H$_2$. From Table 2, among the 84 imines (**Y**), aromatic N-heterocycle **44** (-22.0 kcal mol^{-1}) had the largest thermodynamic driving force to accept H$_2$ producing **44H$_2$**, while the aromatic N-heterocycle **21** (15.8 kcal mol^{-1}) had the smallest thermodynamic driving force to obtain H$_2$ generating **21H$_2$**.

As for the $\Delta G_{H_2A}(Y)$ values, we can safely draw some interesting conclusions to inform the hydrogenation reactions of imines, including aromatic N-heterocycles (**1–78**) and general imines (**79–84**), from Scheme 6. Specifically: (1) for aromatic N-heterocycles, the $\Delta G_{H_2A}(Y)$ scales ranged from -22.0 kcal mol^{-1} to 15.8 kcal mol^{-1} for **Y$_I$**, from -8.5 to 11.5 kcal mol^{-1} for **Y$_{II}$**, and from -9.5 kcal mol^{-1} to 7.4 kcal mol^{-1} for **Y$_{III}$**, respectively. The $\Delta G_{H_2A}(Y)$ scale of aromatic N-heterocycles (**Y$_I$–Y$_{III}$**) ranged from -22.0 kcal mol^{-1} to 15.8 kcal mol^{-1}, which covered a very large range of 37.8 kcal mol^{-1}. The $\Delta G_{H_2A}(Y)$ scales indicated that the H$_2$ (0 kcal mol^{-1}),[22–24] even the great hydrogen-reductant HCO$_2$H (-5.9 kcal mol^{-1}),[25] could not hydrogenate all the aromatic imines (**Y$_I$, Y$_{II}$**, and **Y$_{III}$**) to offer pre-aromatic N-heterocycles (**Y$_I$H$_2$, Y$_{II}$H$_2$**, and **Y$_{III}$H$_2$**). It also could be deduced that some pre-aromatic N-heterocycles from **Y$_I$H$_2$, Y$_{II}$H$_2$**, and **Y$_{III}$H$_2$** were thermodynamically better hydrogen reductants than H$_2$ in hydrogenation reactions. In practice, **27H$_2$** (HEH$_2$),[38–40] **67H$_2$**,[34,35] **73H$_2$**,[41] **74H$_2$**,[42] and **78H$_2$** (ref. 36 and 37) have already
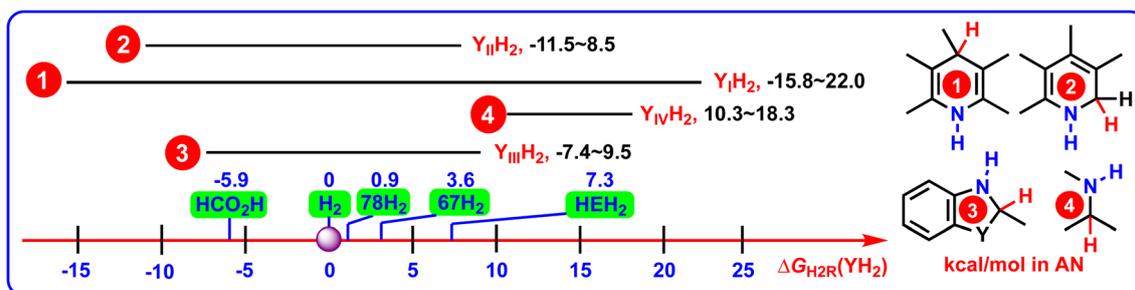
Scheme 5 $\Delta G_{H_2R}(YH_2)$ scales of 4 groups of YH$_2$ (Y$_I$H$_2$–Y$_{IV}$H$_2$), along with the $\Delta G_{H_2R}(XH_2)$ values of HCO$_2$H, H$_2$, 67H$_2$, 78H$_2$, and HEH$_2$ releasing H$_2$ in acetonitrile (kcal mol^{-1}).
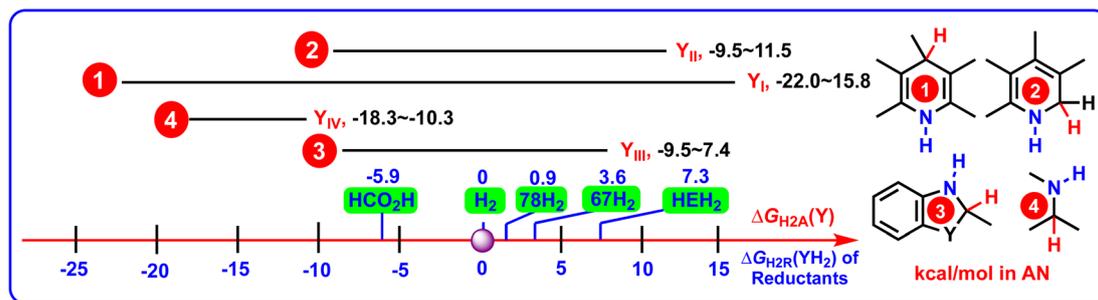
Scheme 6 $\Delta G_{H_2A}(Y)$ scales of 4 groups of Y (Y_I–Y_{IV}), along with the $\Delta G_{H_2R}(XH_2)$ values of HCO_2H, H_2, $67H_2$, $78H_2$, and HEH_2 in acetonitrile (kcal mol^{-1}).

been extensively researched in hydrogenating various unsaturated compounds, including aldehydes ketones, alkenes, imines, and heterocycles;[36–42] (2) in contrast, since Y_{IV} were general imines without aromatic structures, all the $\Delta G_{H_2A}(Y_{IV})$ values (−18.3 to −10.3 kcal mol^{-1}) were all greater than the $\Delta G_{H_2R}(H_2)$ values (0 kcal mol^{-1}), meaning that H_2 could hydrogenate the related general imines (Y_{IV}) in organic synthesis under suitable catalytic conditions, which has been proved by many published studies in the literature.[43–47] Similarly, HCO_2H ($\Delta G_{H_2R}(HCO_2H)$ = −5.9 kcal mol^{-1}),[28] $78H_2$ ($\Delta G_{H_2R}(78H_2)$ = 0.9 kcal mol^{-1}),[36,37] $67H_2$ ($\Delta G_{H_2R}(67H_2)$ = 3.6 kcal mol^{-1}),[34,35] and HEH_2 ($\Delta G_{H_2R}(HEH_2)$ = 7.3 kcal mol^{-1})[38–40] could be applied to hydrogenate Y_{IV} to prepare general amines $Y_{IV}H_2$ in organic synthesis from a thermodynamics viewpoint.

2.3. Thermodynamics for the reversible dehydrogenation and hydrogenation of pre-aromatic and aromatic N-heterocycles

Many groups have focused on the reversible dehydrogenation and hydrogenation of pre-aromatic and aromatic N-heterocycles, mainly including discovering better pre-aromatic N-heterocycles carriers and developing novel metal–organic catalysts.[1–19] Since we have obtained so much valuable thermodynamic data of pre-aromatic N-heterocycles dehydrogenation and aromatic N-heterocycles hydrogenation, it seemed meaningful to clarify why the reversible dehydrogenation and hydrogenation of pre-aromatic and aromatic N-heterocycles could happen, as well as why they possess the typical thermodynamic feature of the corresponding pre-aromatic N-heterocycles.

Theoretically, according to the reaction rule, for the reversible dehydrogenation and hydrogenation of pre-aromatic and aromatic N-heterocycles, if the Gibbs free energy of a YH_2 dehydrogenation ($YH_2 \rightarrow Y + H_2$) is more negative than 0, $\Delta G_{H_2R}(YH_2) < 0$, then the YH_2 dehydrogenation reaction is judged as thermodynamically favorable; while if the Gibbs free energy of the corresponding Y hydrogenation reaction ($Y + H_2 \rightarrow YH_2$) is greater than 0, $\Delta G_{H_2A}(Y) > 0$, then the hydrogenation reaction of Y is thermodynamically unfavorable. In contrast, if the Gibbs free energy of a YH_2 dehydrogenation ($YH_2 \rightarrow Y + H_2$) is greater than 0, $\Delta G_{H_2R}(YH_2) > 0$, and the dehydrogenation

reaction is considered as thermodynamically unfavorable; while if the Gibbs free energy of the corresponding Y hydrogenation ($Y + H_2 \rightarrow YH_2$) is more negative than 0, $\Delta G_{H_2A}(Y) < 0$, and the related Y hydrogenation reaction is regarded as thermodynamically favorable. Therefore, it is very curious why the reversible dehydrogenation and hydrogenation of pre-aromatic and aromatic N-heterocycles could happen, even using the same metal–organic catalyst.[3–9]

Examining the previous literature, it is believed that the H_2 plays a very important role in regulating the reversible dehydrogenation and hydrogenation thermodynamics.[3–9] In YH_2 dehydrogenation, the H_2 is released from the reaction system, which greatly affects the dehydrogenation equilibrium.[3–9] Therefore, the Gibbs free energy of YH_2 dehydrogenation could decrease to make the reaction happen if the $\Delta G_{H_2R}(YH_2)$ value is not too much greater than 0. Furthermore, in Y hydrogenation, the high H_2 pressure would prompt more H_2 to dissolve in the reaction solvent, which would have a strong influence on the hydrogenation equilibrium.[3–9] Consequently, the Gibbs free energy of Y hydrogenation could decrease to make the reaction occur if the $\Delta G_{H_2A}(Y)$ is not too much greater than 0. Herein, this leads to the other key question: what are the restrictions on the $\Delta G_{H_2R}(YH_2)$ value for the reversible dehydrogenation and hydrogenation of a pre-aromatic and aromatic N-heterocycle?[3]

Investigating previous work, the Gibbs solvation energy of H_2 was estimated as 3.4 kcal mol^{-1} in acetonitrile.[48] That is, the Gibbs free energy of H_2 release from acetonitrile solution was −3.4 kcal mol^{-1}, and the H_2 release from the dehydrogenation system could decrease the $\Delta G_{H_2R}(YH_2)$ by 3.4 kcal mol^{-1}. Therefore, it is reasonable to deduce that if the $\Delta G_{H_2R}(YH_2)$ value of a pre-aromatic N-heterocycle is greater than −3.5 kcal mol^{-1} and more negative than 3.5 kcal mol^{-1}, −3.5 kcal mol^{-1} < $\Delta G_{H_2R}(YH_2)$ < 3.5 kcal mol^{-1}, the pre-aromatic N-heterocycle could be considered as a potentially reversible chemical organic hydrogen material, which could release H_2 and be regenerated by H_2 too. According to the above judgment criterion, the $\Delta G_{H_2R}(YH_2)$ values of general amines ($Y_{IV}H_2$) (10.3–18.3 kcal mol^{-1}) are much greater than 3.5 kcal mol^{-1}, and so $Y_{IV}H_2$ could not be designed as reversible dehydrogenation and hydrogenation materials, which is proved by published works.[3–9] Moreover, the $\Delta G_{H_2R}(YH_2)$ scale of 28 pre-aromatic N-heterocycles from Y_IH_2, $Y_{II}H_2$, and $Y_{III}H_2$ ranged from

-3.5 kcal mol^{-1} to 3.5 kcal mol^{-1}, while the corresponding 28 pre-aromatic N-heterocycles were identified as reversible dehydrogenation and hydrogenation materials. The 28 pre-aromatic N-heterocycles included **6H$_2$** (-0.4 kcal mol^{-1}), **7H$_2$** (-0.8 kcal mol^{-1}), **8H$_2$** (2.9 kcal mol^{-1}), **15H$_2$** (2.7 kcal mol^{-1}), **23H$_2$** (-1.9 kcal mol^{-1}), **24H$_2$** (0.6 kcal mol^{-1}), **29H$_2$** (1.9 kcal mol^{-1}), **30H$_2$** (-0.2 kcal mol^{-1}), **31H$_2$** (3.5 kcal mol^{-1}), **32H$_2$** (-0.1 kcal mol^{-1}), **38H$_2$** (0.7 kcal mol^{-1}), **40H$_2$** (2.8 kcal mol^{-1}), **41H$_2$** (0.8 kcal mol^{-1}), **46H$_2$** (-2.5 kcal mol^{-1}), **48H$_2$** (-1.1 kcal mol^{-1}), **49H$_2$** (0.2 kcal mol^{-1}), **51H$_2$** (-0.1 kcal mol^{-1}), **52H$_2$** (-1.3 kcal mol^{-1}), **53H$_2$** (3.0 kcal mol^{-1}), **61H$_2$** (0.3 kcal mol^{-1}), **64H$_2$** (-2.3 kcal mol^{-1}), **65H$_2$** (-1.4 kcal mol^{-1}), **66H$_2$** (1.6 kcal mol^{-1}), **68H$_2$** (2.4 kcal mol^{-1}), **70H$_2$** (0.6 kcal mol^{-1}), **72H$_2$** (1.0 kcal mol^{-1}), **76H$_2$** (2.2 kcal mol^{-1}), and **78H$_2$** (0.9 kcal mol^{-1}), which need further validation and support in experimental work. Examining the chemical structures of the investigated N-heterocycles in previous literature,[3–19] they were not exactly the same pre-aromatic N-heterocycle structure, and most cases involved two H$_2$ molecules release and acceptance from N-heterocycles, which could not provide direct experimental data to validate the thermodynamic model.

2.4. Application of thermodynamic parameters to the selection of pre-aromatic N-heterocyclic hydrogen reductants for catalytic hydrogenation reactions

It is well known that H$_2$ is the greenest hydrogenation reagent with 100% atomic economy.[43–47] Besides H$_2$, the organic hydrogen molecule reductants, most of which are pre-aromatic N-heterocyclics (such as **27H$_2$**, **67H$_2$**, **73H$_2$**, **74H$_2$**, and **78H$_2$**),[36–42] are irreplaceable hydrogen carriers in hydrogenation reactions. Zhou *et al.* developed dual hydrogenation strategies and utilized catalytic amounts of Hantzsch ester (HEH$_2$ or **27H$_2$**)[49] and dihydrophenanthridines (**67H$_2$**)[50] as hydrogen reductants to asymmetrically reduce imines by using H$_2$ as a real reductant for regeneration of the oxidized Hantzsch esters (HE or 27) under a catalyst of metal complexes (Scheme 7). During their work, the reduction of imines, the oxidation of organic hydrogen reductants (pre-aromatic N-heterocycles), as well as the regeneration of oxidized organic hydrogen reductants (aromatic N-heterocycles) all involved H$_2$ transfer. Therefore, the Gibbs free energies for amines dehydrogenation and imines hydrogenation are important thermodynamic parameters to

evaluate the reducing abilities of amines and the hydrogenation difficulties of imines, which could help us discover thermodynamically excellent organic hydrogen reductants or chemical hydrogen-storage compounds, choose appropriate hydrogen reductants, especially for catalytic amounts of hydrogen reductants during the hydrogenation of unsaturated substrates.

If an unsaturated substrate (Sub) is hydrogenated to a reduced unsaturated substrate (SubH$_2$), Sub + H$_2$ → SubH$_2$, whose thermodynamic driving force is defined as the Gibbs free energy of an unsaturated substrate (Sub) accepting H$_2$ to afford SubH$_2$ (equal to the opposite of Gibbs free energy of SubH$_2$ releasing H$_2$ to give Sub, SubH$_2$ → Sub + H$_2$), $\Delta G_{H_2A}(\text{Sub}) = -\Delta G_{H_2R}(\text{SubH}_2)$, then the larger the thermodynamic driving force for the pre-aromatic N-heterocycle reductant dehydrogenation, the more favorable the Sub hydrogenation by **YH$_2$**, *i.e.*, Sub + **YH$_2$** → SubH$_2$ + **Y**.[21]

Herein, the applications of thermodynamic parameters on choosing suitable catalytic amounts of pre-aromatic N-heterocycle reductants in hydrogenation reactions are displayed in Scheme 8 to aid a clear discussion.

It should be noted that not all unsaturated substrates hydrogenation reactions could be designed as organic hydrogen-reductant catalytic reactions. For unsaturated substrates (Sub), if the $\Delta G_{H_2R}(\text{SubH}_2)$ values are more negative than -3.5 kcal mol^{-1}, due to the regeneration of aromatic N-heterocycles being impossible ($\Delta G_{H_2R}(\text{YH}_2) < -3.5$ kcal mol^{-1}), the hydrogenation reactions could not be designed as pre-aromatic N-heterocyclic reductant catalyzed reactions. In contrast, if the $\Delta G_{H_2R}(\text{SubH}_2)$ values of unsaturated substrates are greater than 3.5 kcal mol^{-1}, whose thermodynamic driving force scale of SubH$_2$ releasing H$_2$ is denoted as $\Delta G_{H_2R}(\text{SubH}_2)_{\text{min}} \sim \Delta G_{H_2R}(\text{SubH}_2)_{\text{max}}$, then pre-aromatic N-heterocycles with $\Delta G_{H_2R}(\text{YH}_2)$ values more negative than $\Delta G_{H_2R}(\text{SubH}_2)_{\text{min}}$ and greater than -3.5 kcal mol^{-1} can be recognized as potential catalytic pre-aromatic N-heterocycle reductants, that is, -3.5 kcal mol$^{-1} < \Delta G_{H_2R}(\text{YH}_2) < \Delta G_{H_2R}(\text{SubH}_2)_{\text{min}}$. Specially, if 3.5 kcal mol$^{-1} < \Delta G_{H_2R}(\text{YH}_2) < \Delta G_{H_2R}(\text{SubH}_2)_{\text{min}}$, then the corresponding pre-aromatic N-heterocycles could be designed as thermodynamically good catalytic hydrogen reductants. If $0 < \Delta G_{H_2R}(\text{YH}_2) < 3.5$ kcal mol^{-1}, the corresponding pre-aromatic N-heterocycles could be designed as thermodynamically better catalytic hydrogen reductants. If -3.5 kcal mol$^{-1} < \Delta G_{H_2R}(\text{YH}_2) < 0$ kcal mol^{-1}, the corresponding pre-aromatic N-heterocycles could be designed as the thermodynamically best catalytic hydrogen reductants. If $\Delta G_{H_2R}(\text{YH}_2) < -3.5$ kcal mol^{-1}, the corresponding pre-aromatic N-heterocycles could be considered thermodynamically very excellent reductants, but they could not be regenerated by H$_2$ and designed as catalytic hydrogen reductants.

Thus, it can be seen that the two new thermodynamic parameters $\Delta G_{H_2R}(\text{YH}_2)$ and $\Delta G_{H_2A}(\text{Y})$ can not only help us evaluate and identify good chemical hydrogen-storage materials, but also choose appropriate hydrogen reductants, especially for catalytic amounts of N-heterocyclic hydrogen reductants during the hydrogenation of unsaturated substrates.
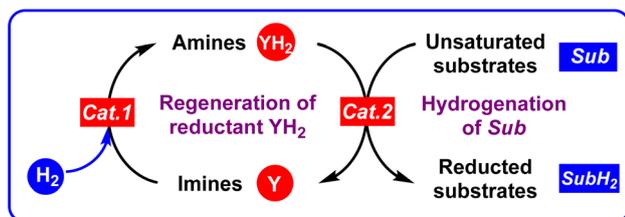
Scheme 7 Dual hydrogenation strategies involving utilizing catalytic amounts of pre-aromatic N-heterocycles as hydrogen reductants to asymmetrically reduce imines by using H$_2$ as a real reductant for the regeneration of aromatic N-heterocycles.
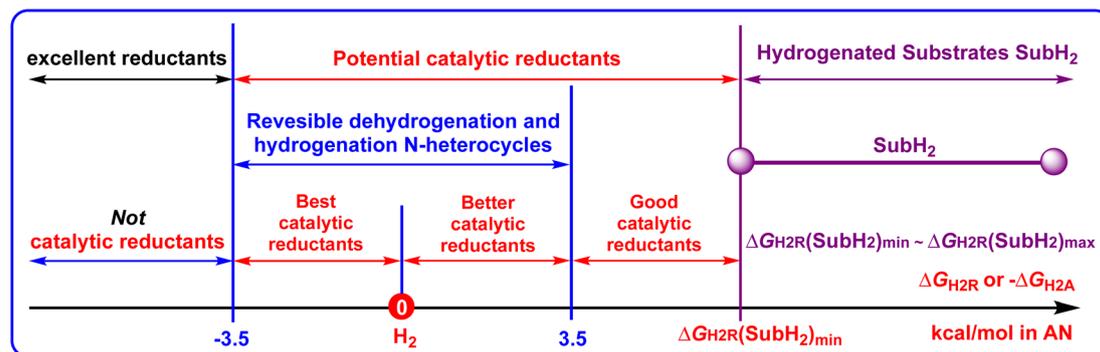
Scheme 8 Applications of the thermodynamic parameters on choosing suitable catalytic amounts of N-heterocyclic hydrogen reductants in hydrogenation reactions.

3 Conclusions

In this work, the Gibbs free energies of pre-aromatic N-heterocycles ($\mathbf{YH_2}$) dehydrogenation and corresponding aromatic N-heterocycles ($\mathbf{Y}$) hydrogenation, $\Delta G_{H_2R}(\mathbf{YH_2})$ and $\Delta G_{H_2A}(\mathbf{Y})$, were derived by constructing thermodynamic cycles using Hess' law. The thermodynamic abilities on the acceptorless dehydrogenation and hydrogenation of 78 pre-aromatic N-heterocycles ($\mathbf{YH_2}$) and related 78 aromatic N-heterocycles ($\mathbf{Y}$) were well evaluated and discussed in acetonitrile. Several valuable conclusions could be drawn as follows:

(1) $\Delta G_{H_2R}(\mathbf{YH_2})$ is an important thermodynamic parameter to guide chemists to discover more potentially excellent hydrogen carriers. Not all pre-aromatic N-heterocycles are thermodynamically feasible chemical hydrogen-storage materials. The $\Delta G_{H_2R}(\mathbf{YH_2})$ scale of the considered 78 pre-aromatic N-heterocycles ranged from -15.8 kcal mol^{-1} to 22.0 kcal mol^{-1}, with 30 $\Delta G_{H_2R}(\mathbf{YH_2})$ values being more negative than 0, meaning that the related 30 $\mathbf{YH_2}$ were identified as thermodynamically feasible H_2 donors, and belong to potential chemical hydrogen-storage materials. The $\Delta G_{H_2R}(\mathbf{Y_IH_2})$ scale (-15.8 to 22.0 kcal mol^{-1}) spanned the widest thermodynamic range by 37.8 kcal mol^{-1} among $\mathbf{Y_IH_2}$–$\mathbf{Y_{IV}H_2}$, and the dehydrogenation abilities of $\mathbf{Y_{II}H_2}$–$\mathbf{Y_{IV}H_2}$ decreased in the order of $\mathbf{Y_{II}H_2} \approx \mathbf{Y_{III}H_2} > \mathbf{Y_{IV}H_2}$.

(2) As for the thermodynamic abilities of $\mathbf{Y}$ hydrogenation, the $\Delta G_{H_2A}(\mathbf{Y})$ data indicated that for H_2, even the great hydrogen-reductant HCO$_2$H (-5.9 kcal mol^{-1}), could not hydrogenate all the aromatic imines ($\mathbf{Y_I}$, $\mathbf{Y_{II}}$, and $\mathbf{Y_{III}}$) to form pre-aromatic N-heterocycles. $\mathbf{Y_{IV}}$ are general imines without aromatic structures, and all their $\Delta G_{H_2A}(\mathbf{Y_{IV}})$ values (-18.3 to -10.3 kcal mol^{-1}) were greater than $\Delta G_{H_2R}(H_2)$ (0 kcal mol^{-1}), meaning that H_2 could hydrogenate the related general imines ($\mathbf{Y_{IV}}$) in organic synthesis under suitable catalytic conditions.

(3) H_2 plays an important role in regulating reversible dehydrogenation and hydrogenation thermodynamics. The thermodynamic features in the reversible dehydrogenation and hydrogenation of pre-aromatic and aromatic N-heterocycles were clarified such that if -3.5 kcal mol^{-1} < $\Delta G_{H_2R}(\mathbf{YH_2})$ < 3.5 kcal mol^{-1}, the pre-aromatic N-heterocycle is considered as a thermodynamically potential reversible chemical organic

hydrogen material, which could release H_2 and be regenerated by H_2 too.

(4) The application of thermodynamic parameters to the selection of pre-aromatic N-heterocyclic hydrogen reductants in catalytic hydrogenation was exhibited in this work. If the $\Delta G_{H_2R}(\mathrm{SubH_2})$ values of unsaturated substrates ($\mathrm{SubH_2}$) are greater than 3.5 kcal mol^{-1}, pre-aromatic N-heterocycles with -3.5 kcal mol^{-1} < $\Delta G_{H_2R}(\mathbf{YH_2})$ < $\Delta G_{H_2R}(\mathrm{SubH_2})_{\min}$ could be recognized as thermodynamically potential catalytic reductants. Specially, if 3.5 kcal mol^{-1} < $\Delta G_{H_2R}(\mathbf{YH_2})$ < $\Delta G_{H_2R}(\mathrm{SubH_2})_{\min}$, the related pre-aromatic N-heterocycles could be designed as thermodynamically good catalytic hydrogen reductants. If 0 < $\Delta G_{H_2R}(\mathbf{YH_2})$ < 3.5 kcal mol^{-1}, the related pre-aromatic N-heterocycles could be designed as thermodynamically better catalytic hydrogen reductants. If -3.5 kcal mol^{-1} < $\Delta G_{H_2R}(\mathbf{YH_2})$ < 0 kcal mol^{-1}, the related pre-aromatic N-heterocycles could be designed as the thermodynamically best catalytic hydrogen reductants.

In summary, this work focused on two new thermodynamic parameters, namely $\Delta G_{H_2R}(\mathbf{YH_2})$ and $\Delta G_{H_2A}(\mathbf{Y})$, which is an important supplement to our previous work to offer precise insights into the chemical hydrogen storage of pre-aromatic N-heterocycles, and hydrogenation reactions.

Conflicts of interest

There are no conflicts of interest to declare.

Acknowledgements

References

1 F. Li, L. Lu and P. Liu, Acceptorless Dehydrogenative Coupling of o-Aminobenzamides with the Activation of Methanol as a C1 Source for the Construction of Quinazolinones, *Org. Lett.*, 2016, **18**, 2580–2583.

2 C. Li, S. Zhang, S. Li, Y. Feng and Q.-H. Fan, Ruthenium-Catalyzed Enantioselective Hydrogenation of Quinoxalinones and Quinazolinones, *Org. Chem. Front.*, 2022, **9**, 400–406.

3 R. Xu, S. Chakraborty, H. Yuan and W. D. Jones, Acceptorless, Reversible Dehydrogenation and Hydrogenation of N-Heterocycles with a Cobalt Pincer Catalyst, *ACS Catal.*, 2015, **5**, 6350–6354.

4 M. G. Manas, L. S. Sharninghausen, E. Lin and R. H. Crabtree, Iridium Catalyzed Reversible Dehydrogenation-Hydrogenation of Quinoline Derivatives under Mild Conditions, *J. Organomet. Chem.*, 2015, **792**, 184–189.

5 R. Yamaguchi, C. Ikeda, Y. Yoshinor Takahashi and K. Fujita, Homogeneous Catalytic System for Reversible Dehydrogenation-Hydrogenation Reactions of Nitrogen Heterocycles with Reversible Interconversion of Catalytic Species, *J. Am. Chem. Soc.*, 2009, **131**, 8410–8412.

6 S. Chakraborty, W. W. Brennessel and W. D. Jones, A Molecular Iron Catalyst for the Acceptorless Dehydrogenation and Hydrogenation of N-Heterocycles, *J. Am. Chem. Soc.*, 2014, **136**, 8564–8567.

7 B. Sawatlon and P. Surawatanawong, Mechanisms for Dehydrogenation and Hydrogenation of N-Heterocycles using PNP-Pincer-Supported Iron Catalysts: A Density Functional Study, *Dalton Trans.*, 2016, **45**, 14965–14978.

8 N. O. Balayeva, Z. Mamiyev, R. Dillert, N. Zheng and D. W. Bahnemann, Rh/TiO$_2$-Photocatalyzed Acceptorless Dehydrogenation of N-Heterocycles upon Visible-Light Illumination, *ACS Catal.*, 2020, **10**, 5542–5553.

9 S. Muthaiah and S. H. Hong, Acceptorless and Base-Free Dehydrogenation of Alcohols and Amines using Ruthenium-Hydride Complexes, *Adv. Synth. Catal.*, 2012, **354**, 3045–3053.

10 I. Dutta, S. Yadav, A. Sarbajna, S. De, M. Hölscher, W. Leitner and J. K. Bera, Double Dehydrogenation of Primary Amines to Nitriles by a Ruthenium Complex Featuring Pyrazole Functionality, *J. Am. Chem. Soc.*, 2018, **140**, 8662–8666.

11 M. Kannan and S. Muthaiah, Extending the Chemistry of Hexamethylenetetramine in Ruthenium-Catalyzed Amine Oxidation, *Organometallics*, 2019, **38**, 3560–3567.

12 R. H. Crabtree, Hydrogen Storage in Liquid Organic Heterocycles, *Energy Environ. Sci.*, 2008, **1**, 134–138.

13 R. King, A. J. Canty, A. Ariafard, R. A. J. O'Hair and V. Ryzhov, Catalytic Dehydrogenation of Liquid Organic Hydrogen Carrier Model Compounds by CpM$^+$ (M = Fe, Co, Ni) in the Gas Phase, *Organometallics*, 2022, **41**, 3823–3833.

14 O. R. Luca, D. L. Huang, M. K. Takase and R. H. Crabtree, Redox-Active Cyclopentadienyl Ni Complexes with Quinoid N-Heterocyclic Carbene Ligands for the Electrocatalytic Hydrogen Release from Chemical Fuels, *New J. Chem.*, 2013, **37**, 3402–3405.

15 H. Y. Zhao, S. T. Oyama and E. D. Naeemi, Hydrogen Storage Using Heterocyclic Compounds: The Hydrogenation of 2-Methylthiophene, *Catal. Today*, 2010, **149**, 172–184.

16 S. M. Bellows, S. Chakraborty, J. B. Gary, W. D. Jones and T. R. Cundari, An Uncanny Dehydrogenation Mechanism: Polar Bond Control over Stepwise or Concerted Transition States, *Inorg. Chem.*, 2017, **56**, 5519–5524.

17 X. Cui, Y. Li, S. Bachmann, M. Scalone, A.-E. Surkus, K. Junge, C. Topf and M. Beller, Synthesis and Characterization of Iron−Nitrogen-Doped Graphene/Core−Shell Catalysts: Efficient Oxidative Dehydrogenation of N-Heterocycles, *J. Am. Chem. Soc.*, 2015, **137**, 10652–10658.

18 D. Zhang, L.-Z. Wu, L. Zhou, X. Han, Q.-Z. Yang, L.-P. Zhang and C.-H. Tung, Photocatalytic Hydrogen Production from Hantzsch 1,4-Dihydropyridines by Platinum(II) Terpyridyl Complexes in Homogeneous Solution, *J. Am. Chem. Soc.*, 2004, **126**, 3440–3441.

19 A. Moores, M. Poyatos, Y. Luo and R. H. Crabtree, Catalysed Low Temperature H$_2$ Release from Nitrogen Heterocycles, *New J. Chem.*, 2006, **30**, 1675–1678.

20 (*a*) Y. Li and X.-Q. Zhu, Theoretical Prediction of Activation Free Energies of Various Hydride Self-Exchange Reactions in Acetonitrile at 298 K, *ACS Omega*, 2018, **3**, 872–885; (*b*) G.-B. Shen, B.-C. Qian, G.-Z. Luo, Y.-H. Fu and X.-Q. Zhu, Thermodynamic Evaluations of Amines as Hydrides or Two Hydrogen Ions Reductants, and Imines as Protons or Two Hydrogen Ions Acceptors, as well as Their Application in Hydrogenation Reactions, *ACS Omega*, 2023, **8**, 31984–31997.

21 G.-B. Shen, B.-C. Qian, Y.-H. Fu and X.-Q. Zhu, Discovering and Evaluating the Reducing Abilities of Polar Alkanes and Related Family Members as Organic Reductants Using Thermodynamics, *J. Org. Chem.*, 2022, **87**, 9357–9374.

22 E. S. Wiedner, M. B. Chambers, C. L. Pitman, R. M. Bullock, A. J. M. Miller and A. M. Appel, Thermodynamic Hydricity of Transition Metal Hydrides, *Chem. Rev.*, 2016, **116**, 8655–8692.

23 K. R. Brereton, N. E. Smith, N. Hazari and A. J. M. Miller, Thermodynamic and Kinetic Hydricity of Transition Metal Hydrides, *Chem. Soc. Rev.*, 2020, **49**, 7929–7948.

24 R. G. Agarwal, C. F. Wise, J. J. Warren and J. M. Mayer, Correction to Thermochemistry of Proton-Coupled Electron Transfer Reagents and its Implications, *Chem. Rev.*, 2022, **122**, 1482.

25 G.-B. Shen, B.-C. Qian, G.-S. Zhang, G.-Z. Luo, Y.-H. Fu and X.-Q. Zhu, Thermodynamics Regulated Organic Hydride/Acid Pairs as Novel Organic Hydrogen Reductants, *Org. Chem. Front.*, 2022, **9**, 6833–6848.

26 G.-B. Shen, B.-C. Qian, Y.-H. Fu and X.-Q. Zhu, Thermodynamics of the Elementary Steps of Organic Hydride Chemistry Determined in Acetonitrile and their Applications, *Org. Chem. Front.*, 2022, **9**, 6001–6062.

27 G.-B. Shen, Y.-H. Fu and X.-Q. Zhu, Thermodynamic Network Cards of Hantzsch Ester, Benzothiazoline, and Dihydrophenanthridine Releasing Two Hydrogen Atoms or Ions on 20 Elementary Steps, *J. Org. Chem.*, 2020, **85**, 12535–12543.

28 D. Wei and C. Darcel, Iron Catalysis in Reduction and Hydrometalation Reactions, *Chem. Rev.*, 2019, **119**, 2550–2610.

29 H. Wang, J. Wen and X. Zhang, Chiral Tridentate Ligands in Transition Metal-Catalyzed Asymmetric Hydrogenation, *Chem. Rev.*, 2021, **121**, 7530–7567.

30 M. Luneau, J. S. Lim, D. A. Patel, E. C. H. Sykes, C. M. Friend and P. Sautet, Guidelines to Achieving High Selectivity for The Hydrogenation of α,β-Unsaturated Aldehydes with Bimetallic and Dilute Alloy Catalysts: A Review, *Chem. Rev.*, 2020, **120**, 12834–12872.

31 Z. Zhang, N. A. Butt and W. Zhang, Asymmetric Hydrogenation of Nonaromatic Cyclic Substrates, *Chem. Rev.*, 2016, **116**, 14769–14827.

32 F. Meemken and A. Baiker, Recent Progress in Heterogeneous Asymmetric Hydrogenation of C=O and C=C Bonds on Supported Noble Metal Catalysts, *Chem. Rev.*, 2017, **117**, 11522–11569.

33 J.-H. Xie, S.-F. Zhu and Q.-L. Zhou, Recent Advances in Transition Metal-Catalyzed Enantioselective Hydrogenation of Unprotected Enamines, *Chem. Soc. Rev.*, 2012, **41**, 4126–4139.

34 B. Gao, W. Meng, X. Feng and H. Du, Regenerable Dihydrophenanthridine via Borane-Catalyzed Hydrogenation for The Asymmetric Transfer Hydrogenation of Benzoxazinones, *Org. Lett.*, 2022, **24**, 3955–3959.

35 J. Wang, Z.-B. Zhao, Y. Zhao, G. Luo, Z.-H. Zhu, Y. Luo and Y.-G. Zhou, Chiral and Regenerable NAD(P)H Models Enabled Biomimetic Asymmetric Reduction: Design, Synthesis, Scope, and Mechanistic Studies, *J. Org. Chem.*, 2020, **85**, 2355–2368.

36 C. Zhu, K. Saito, M. Yamanaka and T. Akiyama, Benzothiazoline: Versatile Hydrogen Donor for Organocatalytic Transfer Hydrogenation, *Acc. Chem. Res.*, 2015, **48**, 388–398.

37 H. Osakabe, S. Saito, M. Miyagawa, T. Suga, T. Uchikura and T. Akiyama, Enantioselective Dehydroxyhydrogenation of 3-Indolylmethanols by The Combined Use of Benzothiazoline and Chiral Phosphoric Acid: Construction of A Tertiary Carbon Center, *Org. Lett.*, 2020, **22**, 2225–2229.

38 C. Zheng and S.-L. You, Transfer Hydrogenation with Hantzsch Esters and Related Organic Hydride Donors, *Chem. Soc. Rev.*, 2012, **41**, 2498–2518.

39 S. G. Ouellet, A. M. Walji and D. W. C. Macmillan, Enantioselective Organocatalytic Transfer Hydrogenation Reactions Using Hantzsch Esters, *Acc. Chem. Res.*, 2007, **40**, 1327–1339.

40 M. Rueping, J. Dufour and F. R. Schoepke, Advances in Catalytic Metal-Free Reductions: from Bioinspired Concepts to Applications in the Organocatalytic Synthesis of Pharmaceuticals and Natural Products, *Green Chem.*, 2011, **13**, 1084–1105.

41 Z.-P. Chen, M.-W. Chen, R.-N. Guo and Y.-G. Zhou, 4,5-Dihydropyrrolo[1,2-*a*]quinoxalines: A Tunable and Regenerable Biomimetic Hydrogen Source, *Org. Lett.*, 2014, **16**, 1406–1409.

42 Y.-S. Feng, C.-Y. Yang, Q. Huang and H.-J. Xu, Study on Comparison of Reducing Ability of Three Organic Hydride Compounds, *Tetrahedron*, 2012, **68**, 5053–5059.

43 A. Cabré, X. Verdaguer and A. Riera, Recent Advances in The Enantioselective Synthesis of Chiral Amines via Transition Metal-Catalyzed Asymmetric Hydrogenation, *Chem. Rev.*, 2022, **122**, 269–339.

44 R. A. A. Abdine, G. Hedouin, F. Colobert and J. Wencel-Delord, Metal-Catalyzed Asymmetric Hydrogenation of C=N Bonds, *ACS Catal.*, 2021, **11**, 215–247.

45 D.-S. Wang, Q.-A. Chen, S.-M. Lu and Y.-G. Zhou, Asymmetric Hydrogenation of Heteroarenes and Arenes, *Chem. Rev.*, 2012, **112**, 2557–2590.

46 J.-D. Yang, J. Xue and J.-P. Cheng, Understanding the Role of Thermodynamics in Catalytic Imine Reductions, *Chem. Soc. Rev.*, 2019, **48**, 2913–2926.

47 X. del Corte, E. M. de Marigorta, F. Palacios, J. Vicario and A. Maestro, An Overview of the Applications of Chiral Phosphoric Acid Organocatalysts in Enantioselective Additions to C=O and C=N bonds, *Org. Chem. Front.*, 2022, **9**, 6331–6399.

48 C. A. Kelly and D. R. Rosseinsky, Estimates of Hydride Ion Stability in Condensed Systems: Energy of Formation and Solvation in Aqueous and Polar-Organic Solvents, *Phys. Chem. Chem. Phys.*, 2001, **3**, 2086–2090.

49 Q.-A. Chen, M.-W. Chen, C.-B. Yu, L. Shi, D.-S. Wang, Y. Yang and Y.-G. Zhou, Biomimetic Asymmetric Hydrogenation: In Situ Regenerable Hantzsch Esters for Asymmetric Hydrogenation of Benzoxazinones, *J. Am. Chem. Soc.*, 2011, **133**, 16432–16435.

50 Q.-A. Chen, K. Gao, Y. Duan, Z.-S. Ye, L. Shi, Y. Yang and Y.-G. Zhou, Dihydrophenanthridine: A New and Easily Regenerable NAD(P)H Model for Biomimetic Asymmetric Hydrogenation, *J. Am. Chem. Soc.*, 2012, **134**, 2442–2448.